

Effect of cathode catalytic and micro-porous layer contact pressure distribution on proton exchange membrane fuel cell cold-start performance

Like Yue¹, Shixue Wang^{1,2*}, Linjun Li¹

¹ School of Mechanical Engineering, Tianjin University, Tianjin, China.

² Key Laboratory of Efficient Utilization of Low and Medium Grade Energy (Tianjin University), Ministry of Education, China.

ABSTRACT

The cold-start performance of proton exchange membrane fuel cells is of great significance to their real-world application. Few experimental studies have investigated the effects of contact pressure distribution on the cold-start performance of fuel cells. In this study, the effects of the changes in the contact pressure distribution between the cathode catalytic layer and the micro-porous layer were experimentally evaluated by varying the channel width of the cathode electrode plate. The output voltage and high-frequency impedance measurements obtained during the cold start of the fuel cell demonstrated that the contact pressure distribution affected the cold-start performance and the effects varied with the temperature. These results indicate that the channel configuration and bolt tightening torque could be manipulated to achieve the best performance under the intended operating conditions.

Keywords: PEMFC, cold start, rib width, channel width, contact pressure distribution

NOMENCLATURE

Abbreviations

PEMFC	Proton Exchange Membrane Fuel Cell
PEM	Proton Exchange Membrane
CL	Catalytic Layer
MPL	Micro-Porous Layer

GDL	Gas Diffusion Layer
<i>Components</i>	
PEM	Nafion 212, 60 μm thick
CL	Platinum load of 0.4 mg/cm^2
GDL	280 μm thick
Channel/Rib	Widths of 0.5 mm/1 mm
Reaction area	25 cm^2

1. INTRODUCTION

Proton exchange membrane fuel cell (PEMFC) provide low operating temperatures, fast start-up and shutdown, and high energy density. These advantages could be beneficially applied to mobile power supplies, vehicles, and other equipment. However, before PEMFC can be adopted for these applications, several issues, such as manufacturing cost, fuel cell life, and cold-start capacity must be addressed. Among these factors, the cold-start performance of fuel cells is highly significant to their practical application. Water generated by the reaction in the cathode catalytic layer (CL) freezes and prevents air from entering the CL, resulting in an insufficient air supply that prevents the PEMFC from starting. Therefore, a PEMFC powered vehicle would not be usable in these conditions. Jiao et al. [1] simulated fuel cell cold start-up and found that icing in

Selection and peer-review under responsibility of the scientific committee of CUE2020

Copyright © 2020 CUE

the channel and gas diffusion layer (GDL) led to a large air pressure drop in the cathode channel. They speculated that cold-start failures were typically caused by the cathode CL freezing. Stahl et al. conducted cold-start experiments on fuel cells at $-2.5\text{ }^{\circ}\text{C}$ and $-10\text{ }^{\circ}\text{C}$ and used neutron imaging technology to study the effects of local icing [2], initial conditions, and residual water [3] on cold-start performance. Yan et al. [4] found that, once the cold start failed, ice in the fuel cell caused the GDL carbon fibers to break, and the CL and proton exchange membrane (PEM) separated, which negatively impacted fuel cell durability. Therefore, the cold-start performance of fuel cells requires substantial improvement.

Through a visualization-based study, Ishikawa et al. [5] found that when the PEMFC temperature was $-10\text{ }^{\circ}\text{C}$ during the cold-start process, the reaction generated super-cooled water that could migrate into the CL and GDL of the cathode. The water could remain super-cooled in a CL having a very small pore diameter, while it froze when it moved from the CL to the interface between the CL and GDL. Aoyama et al. [6] and Tabe et al. [7] also found that super-cooled water was more likely to freeze in the gap between the CL and microporous layer (MPL). When the gap is small, super-cooled water easily flows into the MPL. Therefore, increasing the capacity of fuel cells to store ice during cold start and to drain the super-cooled water quickly enough could delay freezing. Ko et al. [8] simulated and extended the ice storage capacity of a cathode electrode to the MPL. They designed a dual-function MPL with a catalytic function and controlled the platinum content and polymer proportion of the MPL to increase the ice storage capacity and continuous operation time of a fuel cell at low temperatures. Dursch et al. [9] suggested that the internal freezing of fuel cell electrodes is related not only to the temperature but also the amount and distribution of the water inside the electrodes during the cold-start process. The water movement in the cathode is related to the gap between the cathode CL and MPL, which is substantially impacted by the pressure with which the fuel cell is assembled. Dafalla [10] studied the influence of assembly pressure on characteristics such as the current distribution and fuel cell cold-start performance by establishing a three-dimensional mathematical model. The results demonstrated that increasing the clamping pressure during assembly not only increased ice accumulation in the cathode CL but also caused the

membrane to dehydrate and decreased the cold-start performance.

Many studies have investigated the effect of contact pressure on the water distribution and performance of fuel cells under normal temperatures. However, few studies have addressed the effect of contact pressure on the cold-start performance of fuel cells, and most did not do so experimentally. Therefore, in this study, the influence of the assembly contact pressure on PEMFC cold-start performance at various temperatures and for different assembly torques and plate configurations, was experimentally investigated.

2. MATERIALS AND METHODS

The experimental fuel cell cold-start system is shown in Fig. 1. The fuel cell and gas cooling coil were placed in a cryogenic chamber to simulate cold-start conditions. Cylinders outside the cryogenic chamber supplied the reaction gases (hydrogen and air), which were cooled by cooling coils to the temperature inside the cryogenic chamber. During the experiment, the water remaining in the fuel cell after normal operation would freeze at the low temperature, which would affect cold-start performance and reduce durability [11]. Before the cold-start experiment, the fuel cell was purged with nitrogen for one hour and then placed in the cryogenic chamber. After cooling to the determined temperature, the fuel cell remained frozen for three hours. The fuel cell start-up current density was controlled to be $0.04\text{ A}\cdot\text{cm}^{-2}$ because cold starting is more likely to be successful under low current density conditions [12], and the voltage variations and pressure difference between the cathode inlet and outlet were tested. A high frequency (2500 Hz) signal generated by an Interface5000E electrochemical station was used to measure changes in the ohm impedance because the internal resistance of the fuel cell would rise as it froze. The experiment was performed with the cryogenic chamber in its shutdown state to avoid the influence of mechanical vibration caused by its operation [13].

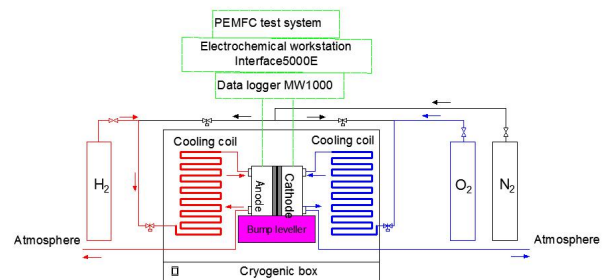


Fig 1 Experimental system.

As shown in Fig. 2, bipolar plates with parallel channels and different rib widths were used in the experiment. The bipolar plate shown in Fig. 2(a) had plate channel and the rib widths of 0.5 mm, and a channel depth of 0.3 mm. The other bipolar plate, shown in Fig. 2 (b), had 1 mm wide plate channels and ribs and a 1 mm channel depth. During the experiment, one bipolar plate, as shown in Fig. 2 (a), served as the anode, and the cathode used both bipolar plates shown in Fig. 2.

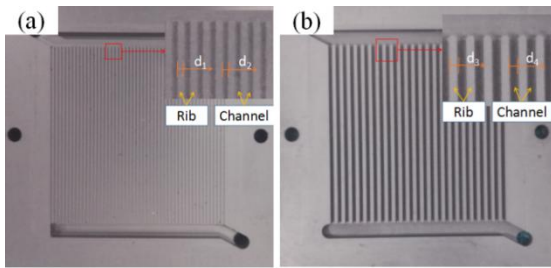


Fig 2 Bipolar plates used in this study with rib widths of (a) 0.5 mm and (b) 1 mm.

If both the CL and MPL are hydrophobic, the water generated by the CL will tend to be retained at the interface between them. In contrast, if they are hydrophilic, the water would be more likely to permeate the porous hydrophilic medium. Therefore, the average contact angles of the surfaces of the tested CLs and MPLs were determined using a contact angle measuring instrument to understand their hydrophilic and hydrophobic characteristics.

If the contact pressure between the CL and MPL is low and the water generated by the CL is at the interface between the CL and MPL, a strongly hydrophobic MPL surface will prevent the water from penetrating it. Further, a water film will form between the two interfaces. Therefore, pressure measuring film was placed at the CL and MPL interface as different torques were applied to the fuel cell fastening bolts to study the influence of pressure and channel width on the contact pressure distribution between the cathode CL and MPL.

3. RESULTS AND DISCUSSION

The contact angle measuring instrument recorded the average contact angle between the surfaces of the CL and MPL to be 128.3° and 140.1°, respectively, indicating that both were hydrophobic. Fig. 3(a), (b), and (c) show the interface contact pressure distributions of the fuel cell cathode CL and MPL when the cathode channel width was 0.5 mm and the applied

torque was 1 N·m, 2 N·m, and 4 N·m, respectively. Fig. 3(d) shows the contact pressure distribution between the cathode CL and MPL when the channel width was 1.0 mm and the bolt torque was 4 N·m. When the bolt torque was 1 N·m and 2 N·m, the pressure was low and the pressure distribution was uneven. In comparison, when the bolt torque was 4 N·m and the channel width was 0.5 mm, the pressure distribution was relatively uniform, as shown in Fig. 3(c). The contact pressure between the CL and MPL under the rib was more than 2.5 MPa, while that under the channel was 1.5–2.25 MPa. When the channel width was 1 mm and the torque was 4 N·m, the pressure distribution under the rib and channel demonstrated greater variation. The contact pressure between the CL and MPL under the rib was more than 2.5 MPa, while that under the channel was between 0.75 and 1.5 MPa.

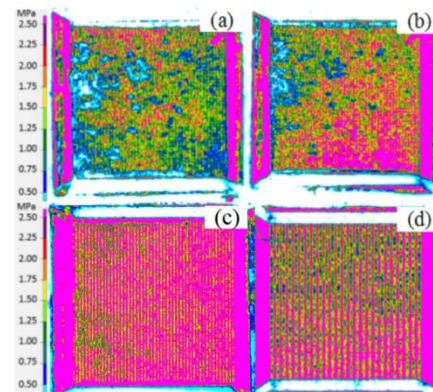


Fig 3 Contact pressure distribution of the cathode CL and MPL for torque values and channel widths of (a) 1 N·m and 0.5 mm, (b) 2 N·m and 0.5 mm, (c) 4 N·m and 0.5 mm, and (d) 4 N·m and 1.0 mm.

As shown in Fig. 3, the assembly pressure and channel width significantly impacted the contact pressure distribution between the cathode CL and MPL. When the fuel cell fastening bolt torque was 4 N·m, the contact pressure distribution was relatively uniform, and the channel width significantly affected the pressure distribution. A fuel cell cold-start experiment was conducted for the cases of the pressure distributions shown in Fig. 3(c) and (d).

The cold-starting temperatures applied were -3 °C, -5 °C, -8 °C, and -10 °C, and the voltage, impedance, and pressure difference between the cathode channel inlet and outlet were measured. Fig. 4 shows the results when the fuel cells with cathode channel widths of 0.5 mm and 1 mm were started at -3 °C and -5 °C, respectively. As shown in Fig. 4(a), under these conditions, the fuel cell with the 0.5 mm wide channel

operated for a longer duration after cold starting than did the fuel cell with a 1 mm channel width. Specifically, at $-3\text{ }^{\circ}\text{C}$, the fuel cells with the 0.5 mm and 1.0 mm wide channels provided stable voltage output for 1650 s and 1200 s, respectively, after which the voltage output dropped to zero. At $-5\text{ }^{\circ}\text{C}$, the operation time of the fuel cell with the 0.5 mm wide channel was approximately 1000 s longer than that with the 1.0 mm wide channel. The cathode inlet and outlet pressure differential was greater when the channel was narrower because, for a given cathode inlet flow rate, the narrow-channeled plate had a smaller cross-sectional flow area that resulted in higher air velocity (Fig. 4(b)). The water generated during the cold start was also more likely to be discharged from the fuel cell. When the channel width was 0.5 mm, the pressure difference between the cathode inlet and outlet began to increase slowly approximately 600 s after cold-starting at $-3\text{ }^{\circ}\text{C}$ and $-5\text{ }^{\circ}\text{C}$. This indicates that the water generated by the CL diffused into the channel after 600 s elapsed. However, with a channel width of 1.0 mm, the cathode inlet and outlet pressure remained constant because the cross-sectional area of flow in the channel was greater. Even if a small amount of water that diffused into the channel were frozen after 600 s, the pressure difference between the cathode inlet and outlet would not increase significantly. 1600 s after cold-starting at $-5\text{ }^{\circ}\text{C}$, the voltage in the fuel cell with the 0.5 mm channel decreased suddenly and the cathode inlet and outlet pressure difference increased sharply due to channel icing.

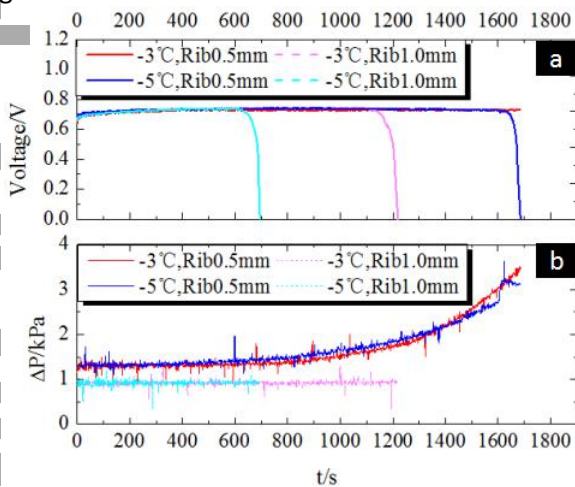


Fig 4 (a) Voltage and (b) pressure difference over time after cold starting at $-3\text{ }^{\circ}\text{C}$ and $-5\text{ }^{\circ}\text{C}$.

Fig. 5 shows the variation of the internal impedance of the fuel cell over time after cold-starting

at $-3\text{ }^{\circ}\text{C}$ and $-5\text{ }^{\circ}\text{C}$. The impedance of the fuel cell with the 0.5 mm wide channel remained stable 600 s after starting at $-3\text{ }^{\circ}\text{C}$, indicating that there was no ice inside the cell, and the diffusion of the liquid water into the channel caused the pressure difference between the cathode inlet and outlet to decrease. In contrast, 1600 s after the fuel cell with the 0.5 mm wide channel was started at $-5\text{ }^{\circ}\text{C}$, the impedance and the pressure difference between the cathode inlet and outlet both suddenly increased, as shown in Fig. 4(b), indicating that internal icing occurred. As can be seen from Fig. 5, when the fuel cell with the 1 mm wide channel was started at $-3\text{ }^{\circ}\text{C}$ and $-5\text{ }^{\circ}\text{C}$, the impedance increased sharply after 600 s and 1000 s, respectively, corresponding to voltage drops that indicated that ice inside the fuel cell caused the cold-start failures. For the fuel cells with channel widths of 0.5 mm and 1 mm started at $-5\text{ }^{\circ}\text{C}$, the fuel cell impedance increased by 1 m Ω and 3 m Ω , respectively. The purging process cannot completely remove all the water from the cell. Icing is more likely to occur in the case of the 1 mm channel because the CL-MPL interface stores water more readily. As shown in Fig. 3, the interface contact between the CL and MPL is closer when the channel is narrow, particularly at the channel location. It could be inferred that the CL and MPL interface contained less water when the channel was narrower. Therefore, the fuel cell with the narrower channel performed better when cold-started because it experienced less of an increase in impedance when it froze than did the fuel cell with the wider channel.

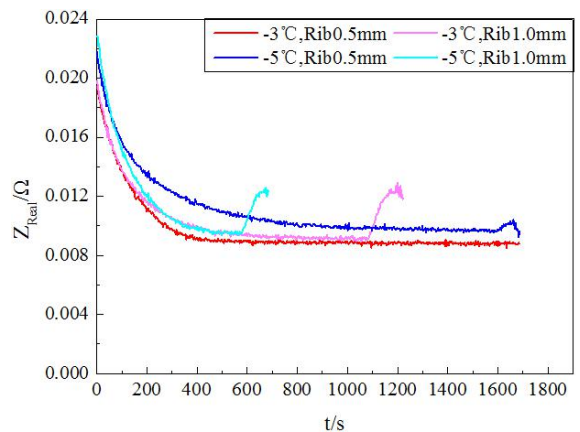


Fig 5 Impedance versus time for cold starts at $-3\text{ }^{\circ}\text{C}$ and $-5\text{ }^{\circ}\text{C}$.

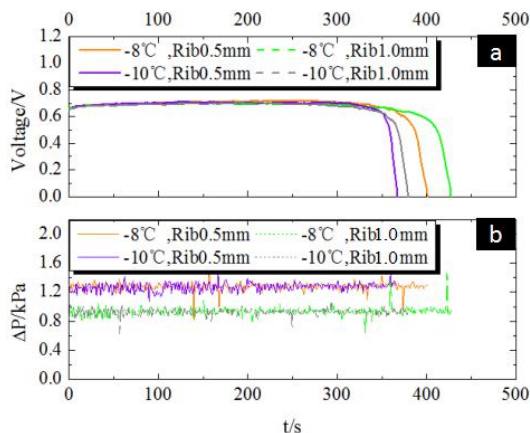


Fig 6 (a) Voltage and (b) pressure difference over time after cold-starting at $-8\text{ }^{\circ}\text{C}$ and $-10\text{ }^{\circ}\text{C}$.

Fig. 6 shows the changes in the fuel cell voltage and the pressure difference between the cathode inlet and outlet when the fuel cell starting temperature was decreased to $-8\text{ }^{\circ}\text{C}$ and $-10\text{ }^{\circ}\text{C}$. Fig. 6(a) illustrates that the fuel cell with the narrower channel provided less operational time than the cell with the wide channel. At $-8\text{ }^{\circ}\text{C}$, the voltage of the fuel cells with channel widths of 1 mm and 0.5 mm began to decrease after 300 s and 375 s, respectively; the corresponding periods over which the voltages dropped to zero were 130 s and 25 s, respectively. The fuel cell with the 1.0 mm channel width experienced the voltage drop sooner and over a longer period. The same trends were also observed after starting the cells at $-10\text{ }^{\circ}\text{C}$. The pressure difference between the fuel cell cathode inlet and outlet remained stable at $-8\text{ }^{\circ}\text{C}$ and $-10\text{ }^{\circ}\text{C}$, indicating that the water produced by the reaction did not diffuse into or freeze in the flow channel. For the same starting current density, the wide channel fuel cell CL became completely covered in ice less quickly than did the narrow channel fuel cell, which had a smaller gap between the CL and MPL. Therefore, when the cold-start temperature was $-8\text{ }^{\circ}\text{C}$ and $-10\text{ }^{\circ}\text{C}$, the water formed by the reaction froze before it could diffuse into the channel.

As shown in Fig. 7, at $-8\text{ }^{\circ}\text{C}$, the impedance of the wide- and narrow-channel fuel cells began to increase after 300 s and 375 s, respectively; with the wider channel, the fuel cell froze more quickly and the impedance increased over a longer duration. Therefore, the use of a wider channel could prolong the duration of the impedance increase. When the starting temperature was $-8\text{ }^{\circ}\text{C}$, the impedance of the narrow- and wide-channel fuel cells began to increase after 350 s and 340 s and increased for approximately 10 s and 35

s, respectively. A comprehensive analysis of Figs. 5 and 7 shows that using narrow-channel plates for the fuel cell cathode could delay the onset of icing during cold-starting. However, at lower starting temperatures, the operational time is longer when the cathode uses a wide channel plate.

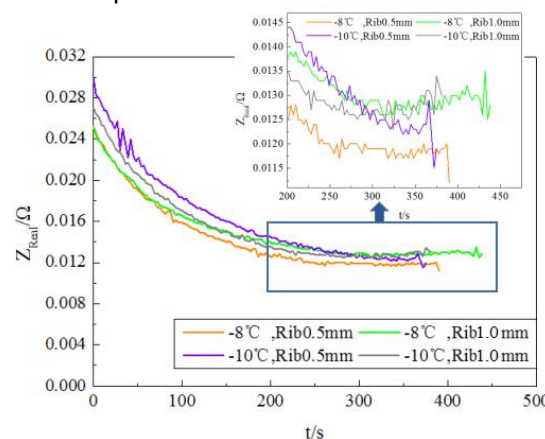


Fig 7 Impedance versus time for cold starts at $-8\text{ }^{\circ}\text{C}$ and $-10\text{ }^{\circ}\text{C}$.

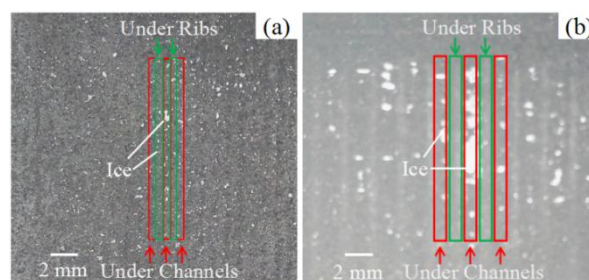


Fig 8 Ice layer distribution on the MPL surface after cold-start failure at $-8\text{ }^{\circ}\text{C}$. Cells pictured had 4 N·m torque applied during assembly and channel widths of (a) 0.5 mm and (b) 1.0 mm.

The ice distribution on the cathode MPL surface after cold-start failure at $-8\text{ }^{\circ}\text{C}$ is shown in Fig. 8. The narrow-channel fuel cell had less ice and a more dispersed ice distribution than the wide-channel fuel cell. Because the contact pressure distribution between the CL and MPL was higher and more uniform, the distribution of the water generated by the electrochemical reaction was also more uniform. In contrast, the ice on the cathode MPL surface of the wide-channel fuel cell was more concentrated and occurred primarily on the surface of the MPL under the channel. When the width of the channel was 1 mm, the contact pressure of the CL and MPL interface under the rib was much higher than that under the channel, thus significantly reducing the porosity of the GDL under the rib. The majority of the electrochemical reaction

occurred in the reaction zone of the channel, and the water produced by the electrochemical reaction was also concentrated in the channel. Further, because the freezing time was longer, the amount of ice was greater.

4. CONCLUSION

In this study, pressure film was used to measure the pressure distribution between the cathode CL and MPL under different fuel cell fastening bolt torques. By changing the width of the cathode channel, the contact pressure distribution between the cathode CL and MPL was varied, and the influence of the pressure distribution on the cold start of the fuel cell was studied.

For the same fuel cell tightening bolt torque, having different channel widths in the cathode plates altered the contact pressure distribution between the CL and MPL, which changed the cold-start performance of the fuel cells at different temperatures. For cold starting at $-3\text{ }^{\circ}\text{C}$ and $-5\text{ }^{\circ}\text{C}$, the fuel cell with the 0.5 mm wide channel started successfully and operated longer than the fuel cell with the 1 mm wide channel. When the fuel cells were started at lower temperatures ($-8\text{ }^{\circ}\text{C}$ and $-10\text{ }^{\circ}\text{C}$), the fuel cell with the 1.0 mm wide channel froze sooner, and the icing process was longer. In contrast, the fuel cell with the 0.5 mm wide channel started icing later, and the icing duration was shorter. These results indicate that the channel configuration and bolt tightening torque could be manipulated to achieve the best performance under the intended operating conditions.

This study provides guidance for fuel cell structure design and optimization of cold start strategy. But a relatively narrow range of temperatures were evaluated and only a few configurations were considered. Future works could expand the number of fuel cell design and construction parameters examined, evaluate the cells at a wider range of temperatures, and assess performance under loading to broaden the applicability of these findings.

ACKNOWLEDGEMENT

This study is supported by the International Cooperation Project (2018YFE0202003) of the Ministry of Science and Technology of China.

REFERENCE

[1] Jiao K, Alaefour I E, Karimi G, et al. Cold start characteristics of proton exchange membrane fuel cells. *Int. J. Hydrog. Energy* 2011; 36(18):11832-11845.

[2] P. Stahl, J. Biesdorf, P. Boillat, et al. An investigation of PEFC sub-zero startup: evidence of local freezing effects. *J. Electrochem. Soc.* 2016; 163 (14): F1535-F1542.

[3] P. Stahl, J. Biesdorf, P. Boillat, et al. An investigation of PEFC sub-zero startup: influence of initial conditions and residual water. *Fuel Cells* 2017; 17(6): 778 – 785.

[4] Yan Q, Toghiani H, Lee Y W, et al. Effect of sub-freezing temperatures on a PEM fuel cell performance, startup and fuel cell components. *J. Power Sources* 2006; 160(2):1242-1250.

[5] Ishikawa Y, Morita T, Nakata K, et al. Behavior of water below the freezing point in PEFCs. *J. Power Sources* 2007; 163:708-712.

[6] Aoyama Y, Suzuki K, Tabe Y, Chikahisa T, Tanuma T. Water transport and PEFC performance with different interface structure between micro-porous layer and catalyst layer. *J. Electrochem. Soc.* 2016; 163: F359-F366.

[7] Tabe Y, Saito M, Fukui K, et al. Cold start characteristics and freezing mechanism dependence on start-up temperature in a polymer electrolyte membrane fuel cell. *J. Power Sources* 2012; 208(2):366-373.

[8] Ko, Johan, Ju, et al. Improving the cold-start capability of polymer electrolyte fuel cells;(PEFCs) by using a dual-function micro-porous layer (MPL): Numerical;simulations[J]. *Int. J. Hydrog. Energy* 2013; 38(1):652-659.

[9] Dursch T J, Ciontea M A, Trigub G J, et al. Ice-Crystallization Kinetics and Water Movement in Gas-Diffusion and Catalyst Layers. *Ecs Transactions* 2013; 50(2):429-435.

[10] A. M. Dafalla, L.Wei, Z. H. Liao, F. M. Jiang. Effects of clamping pressure on cold start behavior of polymer electrolyte fuel cells. *Fuel Cells* 2019; 19(3):221 – 230.

[11] Song K Y, Kim H T. Effect of air purging and dry operation on durability of PEMFC under freeze/thaw cycles. *Int. J. Hydrog. Energy* 2011, 36(19):12417-12426.

[12] Rui L, Weng Y, Yi L, et al. Internal behavior of segmented fuel cell during cold start. *Int. J. Hydrog. Energy* 2014; 39(28):16025-16035.

[13] Takaaki Inada, Xu Zhang, Akira Yabe, et al. Active control of phase change from super cooled water to ice by ultrasonic vibration 1. Control of freezing temperature. *Int. J. Heat Mass Transf.* 2001; 44(23): 4523-4531.